Advances in World Medical Research, 2025, 1(1), 3-17
https://doi.org/10.71204/j7y2f615

Role of BAZ2A in Cervical Cancer and Its Effect on Tumor Cell Metabolism

Jiarui Xue [1], Fenglin Dong [1], Yiwei Liu [1], Shuqing Wang [2,3]*, Fen Hu [1], Bin Zhang [4], Guijie Qi [5], Zhihao Shen [5], Rui Guo [5], Panyan Du [5], Ying Zhang [5], Mingjia Zhao [5], Liyuan Han [5], Linfeng Zhou [5], Jinghua Zhang [2,5,6]*, Yan Liu [1,6]*

[1] College of Life Science, North China University of Science and Technology, Tangshan 063210, China

[2] School of Public Health, North China University of Science and Technology, Tangshan 063210, China

[3] Hospital of North China University of Science and Technology, Tangshan 063210, China

[4] Academic Affairs Department, North China University of Science and Technology, Tangshan 063001, China

[5] Department of Clinical Laboratory, North China University of Science and Technology Affiliated Tangshan Maternal and Child Health Hospital, Tangshan 063000, China.

[6] Hebei Key Laboratory of Molecular Oncology, Tangshan 063001, China

*** Correspondence**:

Wang Shuqing

wsq7992023@163.com

Zhang Jinghua

jhzhang_te@163.com

Liu Yan

liuysm@ncst.edu.cn

Received: 2 April 2025/ Accepted: 12 May 2025/ Published online: 20 May 2025

Abstract

This study aims to investigate the role of BAZ2A in cervical cancer and its relationship with cancer development and glycolipid metabolism. BAZ2A knockdown experiments were performed in HeLa cells to study its effects on cell proliferation, invasion, cloning and migration; transcriptome and metabolome sequencing were also performed, and differentially expressed genes and metabolites were analyzed by GO and KEGG enrichment, etc. BAZ2A is highly expressed in cervical cancer, and the knockdown of BAZ2A inhibits the related malignant behaviors in HeLa cells. Transcriptome analysis identified a large number of differentially - expressed genes and related pathways, while metabolome analysis identified a variety of different

metabolites and related pathways. The joint analysis revealed that key genes and metabolites are involved in the BAZ2A regulatory network, affecting the related signaling pathways. Moreover, BAZ2A plays an important role in cervical cancer development and is closely related to glycolipid metabolism. In conclusion, BAZ2A affects cervical cancer development via cell proliferation, cloning, migration, invasion, and energy metabolism.

Keywords: BAZ2A; Cervical Cancer; Transcriptome; Metabolome; Enrichment Analysis

1. Introduction

Cancer has emerged as a global health problem with a continuously increasing morbidity and mortality (Bray et al., 2018; Sung et al., 2021). The development of tumors involves abnormal genetic and molecular mechanisms (Hanahan & Weinberg, 2011). Despite the advancements in research, the action mechanisms of certain key genes remain unclear (Xu et al., 2020; Johnson et al., 2019). Research on tumors mainly focuses on key genes and their underlying mechanisms. Despite the progress in cancer treatment, drug resistance and side - effects significantly affect the treatment efficacy and prognosis (Siegel et al., 2024). Therefore, investigating the pathogenesis of cancer is of crucial importance for the development of novel therapies to improve prognosis (Li et al., 2021).

BAZ2A serves as an epigenetic regulator that influences ribosomal RNA (rRNA) transcription (Dalle Vedove et al., 2022) and participates in rDNA heterochromatin formation by forming a complex with SNF2H (Bevill et al., 2019; Anosova et al., 2015). The PHD - BRD structural domain of BAZ2A is associated with rDNA silencing (Tallant et al., 2015; Bortoluzzi et al., 2017). BAZ2A promotes tumor invasion and cancer progression (GLi et al., 2018; Gu et al., 2015). Notably, it is highly expressed in prostate cancer, and this high expression is predictive of cancer (Pietrzak et al., 2020). The role of BAZ2A in cancer has been extensively investigated, with a focus on specific cancer types.

Our laboratory has been conducting research on the relationship between the BAZ family and tumors. Previously, we published a series of related research findings on this topic. For instance, "KRASG12 mutant induces the release of the WSTF/NRG3 complex and contributes to an oncogenic paracrine signaling pathway" (Gu et al., 2015) revealed the relationship between KRASG12 mutation and the release of the WSTF/NRG3 complex and its contribution to an oncogenic paracrine signaling pathway. "WSTF acetylation by MOF promotes WSTF activities and oncogenic functions" (Pietrzak et al., 2020) explored the acetylation of WSTF by MOF and its impact on WSTF activities and oncogenic functions. "Pan - cancer and multi - omics analyses revealed the diagnostic and prognostic value of BAZ2A in liver cancer" (Liu et al., 2016) demonstrated the diagnostic and prognostic value of BAZ2A in liver cancer through pan - cancer and multi - omics analyses. These research findings have laid the foundation for a further in - depth investigation of the role of the BAZ family in tumors.

Cervical cancer is one of the major malignant tumors in women and poses a serious health threat. Despite the progress in research, its pathogenesis has not been completely clarified (Liu et al., 2020; Liu et al., 2024). These research findings provide a basis for an in - depth exploration of

the role of the BAZ family in tumors. This study focuses on the role of BAZ2A in cervical cancer. It investigates the effects of BAZ2A on the proliferation, invasion, cloning, and migration of cervical cancer cells, as well as its regulatory mechanisms at the gene - expression and metabolic levels and its association with glycolipid metabolism.

2. Materials and Methods

2.1. Cell Culture

Colon cancer cells SW620, human mammary ductal carcinoma cells HCC38, cervical cancer cells HeLa, and human ovarian cancer cells SKOV3 (STR - validated cells) were kindly provided by Xaar Biological Laboratories (Tianjin, China). Cells were cultured in DMEM medium (Thermo, Waltham, MA, USA) supplemented with 10% FBS (Thermo) in an incubator maintained at 37°C with 5% CO2. SiRNAs (si - NC and si - BAZ2A) obtained from Saier Biotechnology Inc (Tianjin, China) were transfected into cells using Lipofectamine 2000 (Thermo). After a 4 - 6 h incubation in serum - free medium, the cells were then switched to serum - supplemented medium. The sequences of the siRNAs are as follows: si - BAZ2A: 5′ - GAG AGUGUC AGA CUA CUA UTT - 3′ and si - NC: 5′ - UUC UCC GAA CGU GUC ACG UTT - 3′.

2.2. RT-qPCR

The RNA of the cells was extracted using Trizol (Thermo) reagent. The FastKing RT kit (Takara, Chuo - ku, Osaka City, Japan) was used to synthesize cDNA from RNA. The SYBR Premix EX Taq Kit (Takara) was used for RT - PCR analysis. The mRNA level of BAZ2A was quantified using the $2^{-\Delta\Delta CT}$ method, with β - actin mRNA serving as an internal reference. The reaction was conducted under the following conditions: an initial denaturation at 94 °C for 30 s, followed by annealing at 58 °C for 30 s and extension at 72 °C for 30 s. This procedure was repeated 40 times.

The primer sequences used are as follows: For β - actin, sense: 5′ - CGT GAC ATT AAG GAG AAG CTG - 3′, antisense: 5′ - CTA GAA GCA TTT GCG GTG GAC - 3′; for BAZ2A, sense: 5′ - GGA GCA GCG GGT TAT CAT - 3′, antisense: 5′ - CAC AGC CAG GTC CAA AGG - 3′.

2.3. CCK8

After being transfected with siRNA, the cells were inoculated into 96 - well plates at a concentration of 2×10^3 cells per well and then incubated for 24 h. Subsequently, the cells were washed with PBS. The cells were treated with CCK8 reagent (Thermo) and incubated for 2 h. Then, the OD value was measured using a microreader.

2.4. Protein Blotting

After lysing the cells, the protein concentration was measured using the BCA Quantitation Kit (Thermo). Subsequently, an equal amount of protein was separated by 6% SDS - PAGE and then transferred onto a nitrocellulose filter membrane. At room temperature, the membrane was incubated in 3% skim milk for 2 h to block non - specific binding. In this study, since incubating

multiple antibodies simultaneously would interfere with each other, resulting in mixed bands, the membrane was cut and then incubated overnight at 4 °C with specific primary antibodies respectively: BAZ2A (ab290639, Abcam, Cambridge, MA, USA), GADPH (ab8245, Abcam), BAX (ab32503, Abcam), Snail (MA5 - 14801, Thermo), p53 (GTX34938, GeneTex, TX, USA), Bcl - 2 (GTX100064, GeneTex), Vimentin (GTX40346, GeneTex), E - cadherin (CSB - RA576116A0HU, CUSABIO, Wuhan, China), and N - cadherin (CSB - RA243509A0HU, CUSABIO). The membrane was incubated with the corresponding secondary antibody (CSB - PA564648/CSB - PA573747, CUSABIO) for 1 h. The ECL chemiluminescence substrate (PerkinElmer, Waltham, MA, USA) was used to visualize the bands.

2.5. Transwell Assay

A suspension of 1×10^5 cells in 100 μL of serum - free medium was added to the upper chamber of a Transwell apparatus, and 750 μL of serum - containing medium was added to the lower chamber. Three biological replicates were included for each condition. The plates were incubated for 12 - 16 h, and then the chambers were removed. The filter was fixed with 4% paraformaldehyde (BL539A, Biosharp, Beijing, China) and then incubated with 800 μL of 0.5% crystal violet (G1063, Solarbio, Beijing, China) solution for 15 min in the dark. The samples were observed using an inverted microscope. Each sample was randomly examined in five different fields of view, and the number of cells passing through the filtration membrane was counted. For invasion assays, Matrigel (Corning, NY, USA), diluted 1:8 with serum - free medium, was added to the lower chamber and incubated for 5 h in a 37 °C incubator. The cells were then evaluated as described above.

2.6. Clone Formation Assay

Cells were seeded into six - well plates at densities of 50, 100, or 200 cells per well and subsequently cultured for 2 - 3 weeks. After the removal of the medium, the plates were rinsed twice with PBS and subsequently fixed in 5 mL of pure methanol for 15 min. Following the removal of the fixative solution, the cells were stained with 0.4% crystal violet for a duration of 10 - 30 min. The plates were washed, air - dried, and subsequently photographed. The number of colonies was counted to quantify them.

2.7. Transcriptome Sequencing Analysis

Samples were collected using Trizol Reagent (Invitrogen, Carlsbad, CA, USA) at a cell density of 5×10^6 cells per mL. Transcriptome sequencing was conducted by Zhongke New Life Biotechnology Co., Ltd (China).

2.8. Metabolome Sequencing Analysis

The constructed cells were expanded, cultured, and subsequently inoculated into T75 cell - culture flasks, with 6 replicates per group and a cell number of 10^7 or above per sample. Then, cell samples were collected. Metabolome sequencing was conducted by Zhongke New Life Biotechnology Co., Ltd (China).

2.9. Statistical Analysis

Statistical analyses were conducted using GraphPad Prism 8.2.1, and group comparisons were performed via Student's t - test. A P - value of less than 0.05 was regarded as statistically significant.

3. Results

3.1. BAZ2A is Highly Expressed in Cervical Cancer and Promotes Malignant Behaviors of Cervical Cancer Cells

We first detected the expression level of BAZ2A in multiple tumor cell lines by qRT-PCR. Results showed that BAZ2A was most highly expressed in colorectal cancer SW620 cells (Figure. 1A). We then designed siRNAs targeting BAZ2A (si-BAZ2A-1, si-BAZ2A-2, si-BAZ2A-3) and validated their interference efficiency in SW620 cells via qRT-PCR and Western blot. qRT-PCR showed a significant reduction in BAZ2A mRNA levels with si-BAZ2A-2 compared to the control group (si-NC) (Figure. 1B). Western blot further confirmed a marked decrease in BAZ2A protein expression after si-BAZ2A-2 treatment (Figure. 1C), indicating that si-BAZ2A-2 had the optimal interference efficiency.

Given the extensive use of HeLa cells in tumor research due to their unique biological properties and our laboratory's stable culture conditions, we selected HeLa cells with intermediate expression levels for subsequent experiments (Masters, 2002). The effects of BAZ2A on cell proliferation, invasion, colony formation, and migration were analyzed using CCK8, Transwell, colony formation, and scratch wound-healing assays. Knockdown of BAZ2A significantly reduced the proliferative capacity of HeLa cells (Figure. 1D), decreased the number of invasive cells (Figure. 1E), reduced colony formation (Figure. 1F), and shortened migration distance (Figure. 1G). These results collectively indicate that BAZ2A knockdown inhibits proliferation, colony formation, migration, and invasion in HeLa cells.

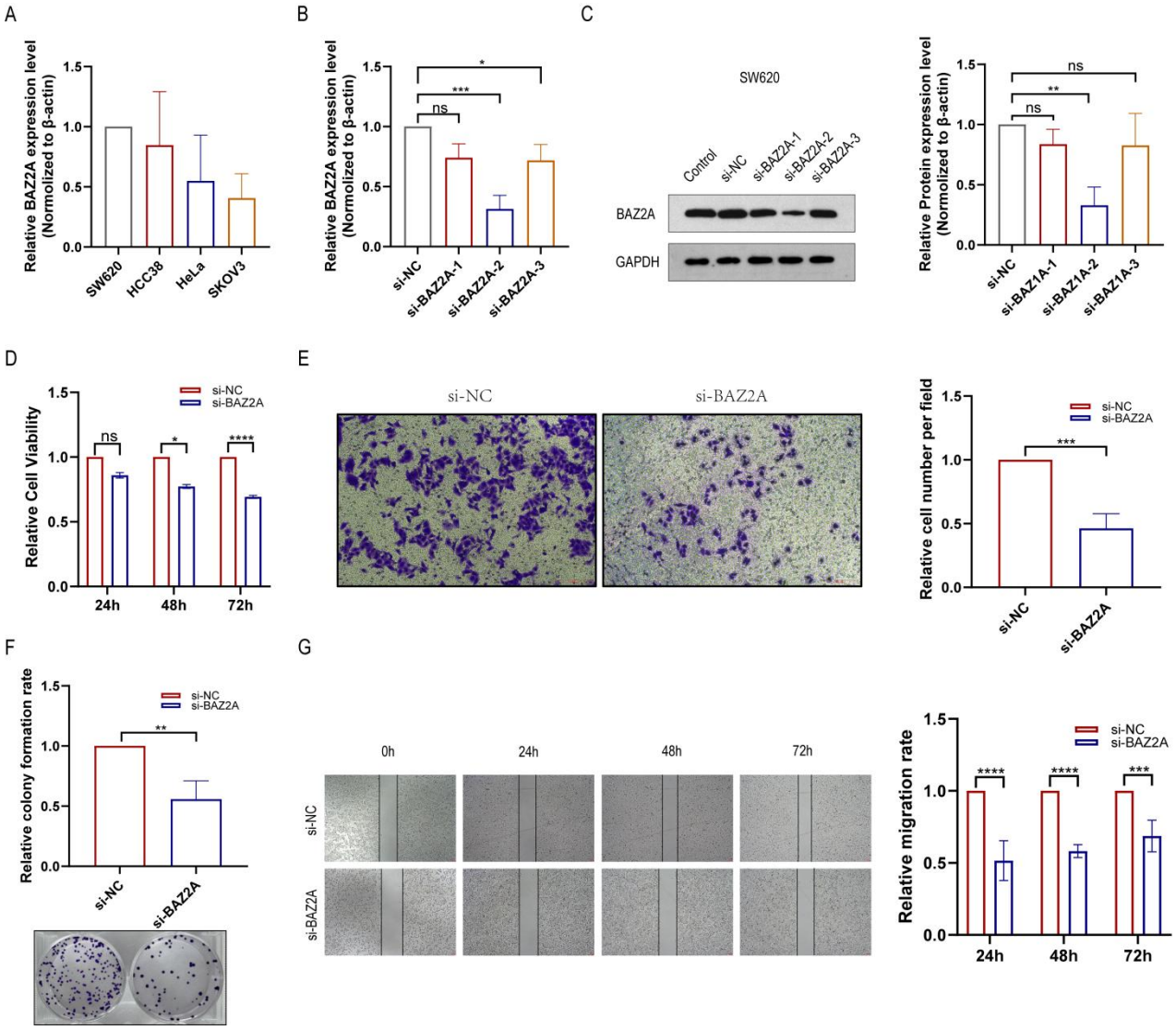


Figure 1. BAZ2A is Upregulated in Cervical Cancer and Promotes Malignant Behaviors in Cervical Cancer Cells

Notes: (A) qRT - PCR Analysis of BAZ2A mRNA Expression in Cervical Cancer Cell Lines. (B) Validation of siRNA Targeting BAZ2A by qRT - PCR in SW620 Cells. (C) Validation of siRNA Targeting BAZ2A by Western Blot in SW620 Cells. (D) The Role of BAZ2A in the Proliferation of HeLa Cells. (E) The Role of BAZ2A in the Invasion of HeLa Cells. (F) The Role of BAZ2A in the Cloning of HeLa Cells. (G) The Role of BAZ2A in the Migration of HeLa Cells. *P < 0.05, **P < 0.005, ***P < 0.001. P - values Less Than 0.05 Were Considered Statistically Significant.

3.2. Transcriptome Analysis of BAZ2A

To investigate the association between BAZ2A and cancer, transcriptome sequencing was performed on cells with BAZ2A knockdown or NC-siRNA transfection. A total of 6,825 differentially expressed genes (DEGs) were identified, including 3,911 upregulated and 2,914 downregulated genes (Figure. 2A). Heatmap analysis showed that DEGs were associated with key processes in tumorigenesis (Figure. 2B).

GO and KEGG enrichment analyses were conducted to annotate DEG functions. GO analysis revealed significant enrichment of 1,689 GO terms ($P < 0.05$), with 81.8% related to biological

processes (BP), including carbohydrate metabolism and lipid metabolic processes (e.g., carbohydrate metabolism, lipid metabolism regulation and transport); 11.6% related to molecular functions (MF), such as anion binding, enzyme binding, and transferase activity; and 6.6% related to cellular components (CC), including plasma membrane, vesicles, ribosomes, and glycogen granules (Liu et al., 2021; Aktary et al., 2017; Stanley, 2011; Jiao et al., 2023; Pecoraro et al., 2021; Neoh et al., 2024) (Figure. 2C-E). These results are illustrated by the directed acyclic plots in Supplementary Figure 1A-C. KEGG analysis showed that DEGs were primarily enriched in tumor progression and metabolic pathways, such as "Pathways in Cancer," "mTOR signaling pathway," and "insulin signaling pathway" (Figure. 2F). the mTOR signaling pathway plays a central role in cellular metabolism (Zou et al., 2020), suggesting that BAZ2A may influence glycolipid metabolism via regulating the mTOR pathway. Detailed information is presented in Supplementary Figure 1D.

Protein-protein interaction network analysis identified ribosomal protein RPS12 as a central node in DEG interactions (Figure. 2G), whose aberrant expression is closely linked to tumorigenesis (Katanaev et al., 2020). Transcription factor annotation revealed enrichment of zf-C2H2 zinc finger proteins, Homeobox, and bHLH family transcription factors in DEGs (Figure. 2H), indicating that BAZ2A may regulate cell differentiation and proliferation by modulating these transcription factors (Zhang et al., 2024; Grier et al., 2005; Putarjunan et al., 2016). Alternative splicing analysis showed that BAZ2A knockdown disrupted mTOR and insulin signaling pathways (Figure. 2I-J), further supporting its role in cellular metabolism and proliferation.

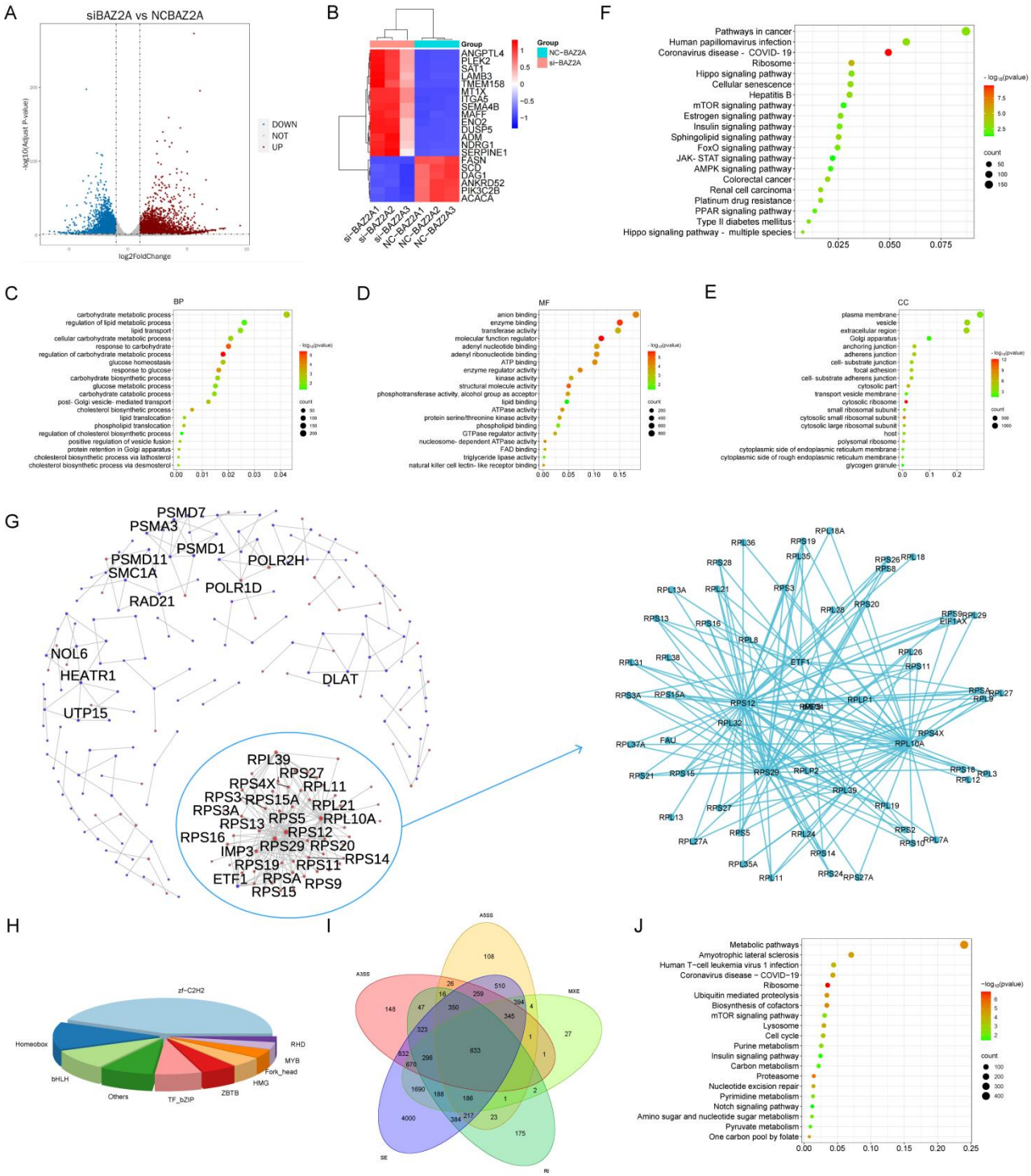


Figure 2. BAZ2A Transcriptome Analysis

Notes: (A) Volcano Plot of Differentially Expressed Genes (DEGs). (B) Heat Map of the Top 20 DEGs. (C - E) GO Enrichment Bubble Diagrams of Differential Genes: (C) Biological Process (BP), (D) Molecular Function (MF), (E) Cellular Component (CC). (F) KEGG Enrichment Bubble Diagram of Differential Genes. (G) Interaction Network Diagram of the Top 300 Differentially Expressed Genes. (H) Pie Chart of Transcription Factor Family Information Statistics. (I) Venn Diagram of Differential Analysis of Alternative Splicing Events (FDR < 0.05 Was Used as the Screening Criterion for Differential AS Events). (J) KEGG Enrichment Bubble Plot of Alternative Splicing Genes.

3.3. Metabolome Analysis of BAZ2A

Metabolome analysis in positive and negative ion modes identified 4,839 (positive ion) and 3,699 (negative ion) differential metabolites, with 1,969/2,870 (positive ion) and 1,464/2,235 (negative ion) metabolites upregulated/downregulated, respectively (Figure. 3A-B). Heatmaps of the top 20 differential metabolites showed their association with tumor development, energy metabolism, and signaling (Figure. 3C-F).

KEGG analysis revealed significant enrichment of differential metabolites in glycolipid metabolism pathways, such as "Central Carbon Metabolism in Cancer" and "Citrate Cycle (TCA Cycle)" (Figure. 3G). Further analysis showed that BAZ2A knockdown enhanced glycolytic activity while inhibiting pyruvate conversion into the TCA cycle, leading to truncation of mitochondrial TCA cycle. Citrate was redirected to extramitochondrial fatty acid synthesis, restricting cis-aconitic acid and isocitric acid synthesis—although isocitric acid accumulated due to upstream substrate buildup. Fumarate synthase dysfunction blocked malate production from fumarate, causing fumarate accumulation (Figure. 3H). These metabolic alterations collectively promoted abnormal cell proliferation and metabolic reprogramming, providing a metabolic basis for cancer cell energy demands.

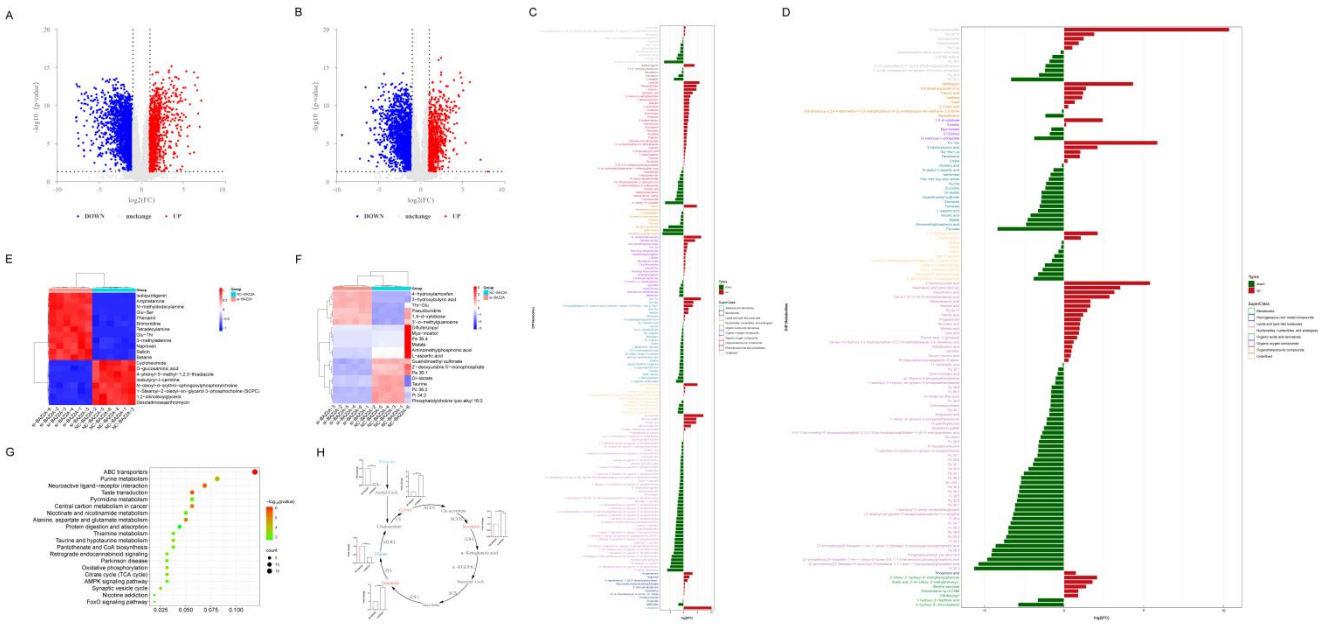


Figure 3. BAZ2A Metabolome Analysis

Notes: (A) Volcano Plot of Differential Metabolites in the Positive Ion Mode (FC > 1.5 or FC < 0.67, P - value < 0.05). (B) Volcano Plot of Differential Metabolites in the Negative Ion Mode (FC > 1.5 or FC < 0.67, P - value < 0.05). (C) Fold - Change Analysis of Significant Differential Metabolites in the Positive Ion Mode. (D) Fold - Change Analysis of Significant Differential Metabolites in the Negative Ion Mode. (E) Heat Map of the Top 20 Differential Metabolites in the Positive Ion Mode. (F) Heat Map of the Top 20 Differential Metabolites in the Negative Ion Mode. (G) KEGG Enrichment Bubble Diagram of Differential Metabolites. (H) The Tricarboxylic Acid Cycle Pathway with Intermediate Metabolites and Response - Regulating Enzymes. Up - regulated Differential Metabolites Are Shown in Red, Down - regulated Metabolites Are Shown in Blue, and Metabolites with Insignificant Changes Are Shown in Black. The Bar Graphs Represent the Statistical Plots of the Metabolites with Significant Differences. *P < 0.05, **P < 0.005, ***P < 0.001. P - values Less Than 0.05 Were Considered Statistically Significant.

3.4. Joint Analysis of Transcriptome and Metabolome for BAZ2A

The PCA plots of Figure 4A, B showed reliable reproducibility. Analysis of the Venn diagram (Figure 4C) revealed that 338 and 154 differentially expressed genes and metabolites were involved in the pathway in the transcriptome and metabolome, respectively, of which six were shared. This finding indicates that there are co - regulated genes and metabolites under BAZ2A regulation. Analysis demonstrated that among the top 10 pathways jointly involved by the transcriptome and metabolome, the “cAMP signaling pathway” (with “cAMP” being cyclic adenosine monophosphate) was highly implicated. This suggests that BAZ2A may synergistically regulate gene expression and metabolism via this pathway, thereby influencing cell physiological processes (Figure 4D). Following the knockdown of BAZ2A, the AMPK, FoxO, and mTOR signaling pathways were affected. This implies that BAZ2A plays a role in cellular energy metabolism and tumor development. Moreover, BAZ2A may indirectly regulate glucose and lipid metabolism by influencing these signaling pathways, which subsequently impact tumor development (Figure 4E).

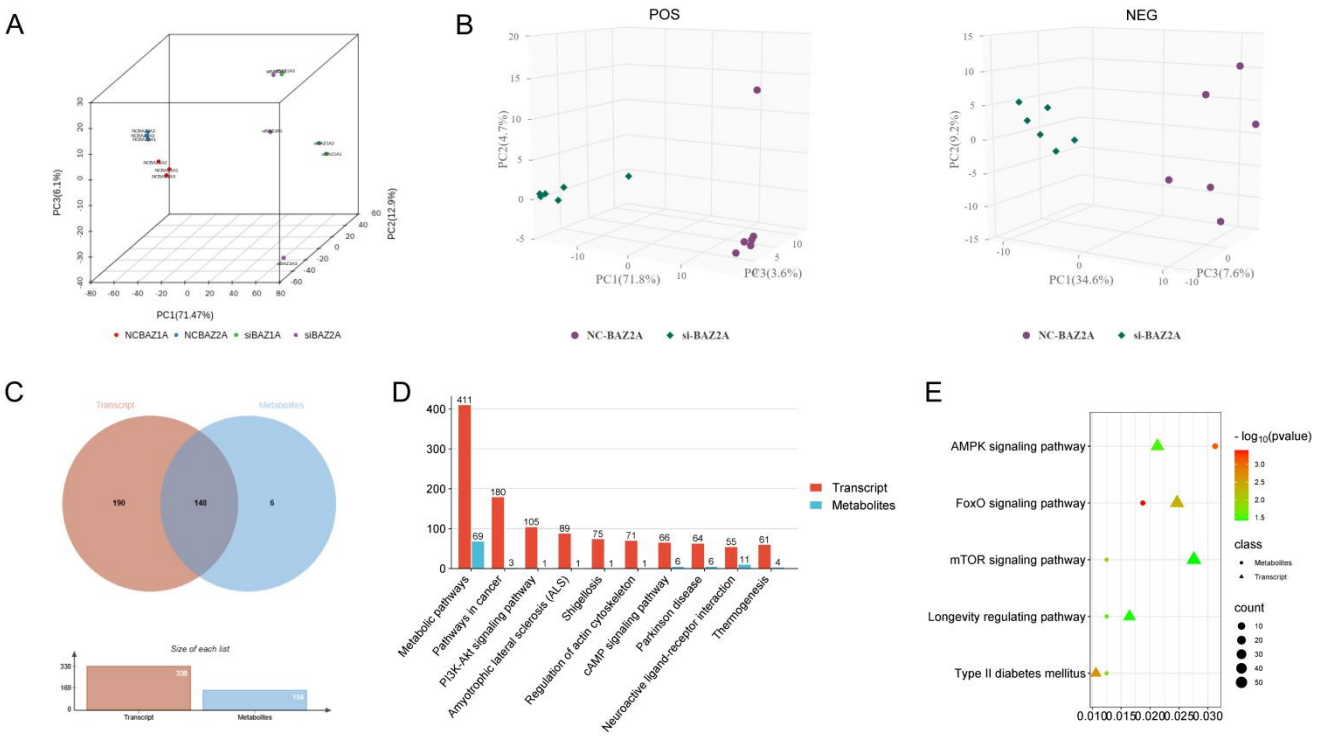


Figure 4. Joint Metabolome and Transcriptome Analysis of BAZ2A

Notes: (A) PCA Plots of Differentially Expressed Genes. (B) PCA Plots of Differential Metabolites. (C) Venn Diagram of Differentially Expressed Genes and Differential Metabolites Involved in the Pathways. (D) The Top 10 Pathways with the Highest Number of Jointly Involved Genes and Metabolites. (E) KEGG Enrichment Bubble Plot of Differential Genes Versus Differential Metabolites.

4. Discussion

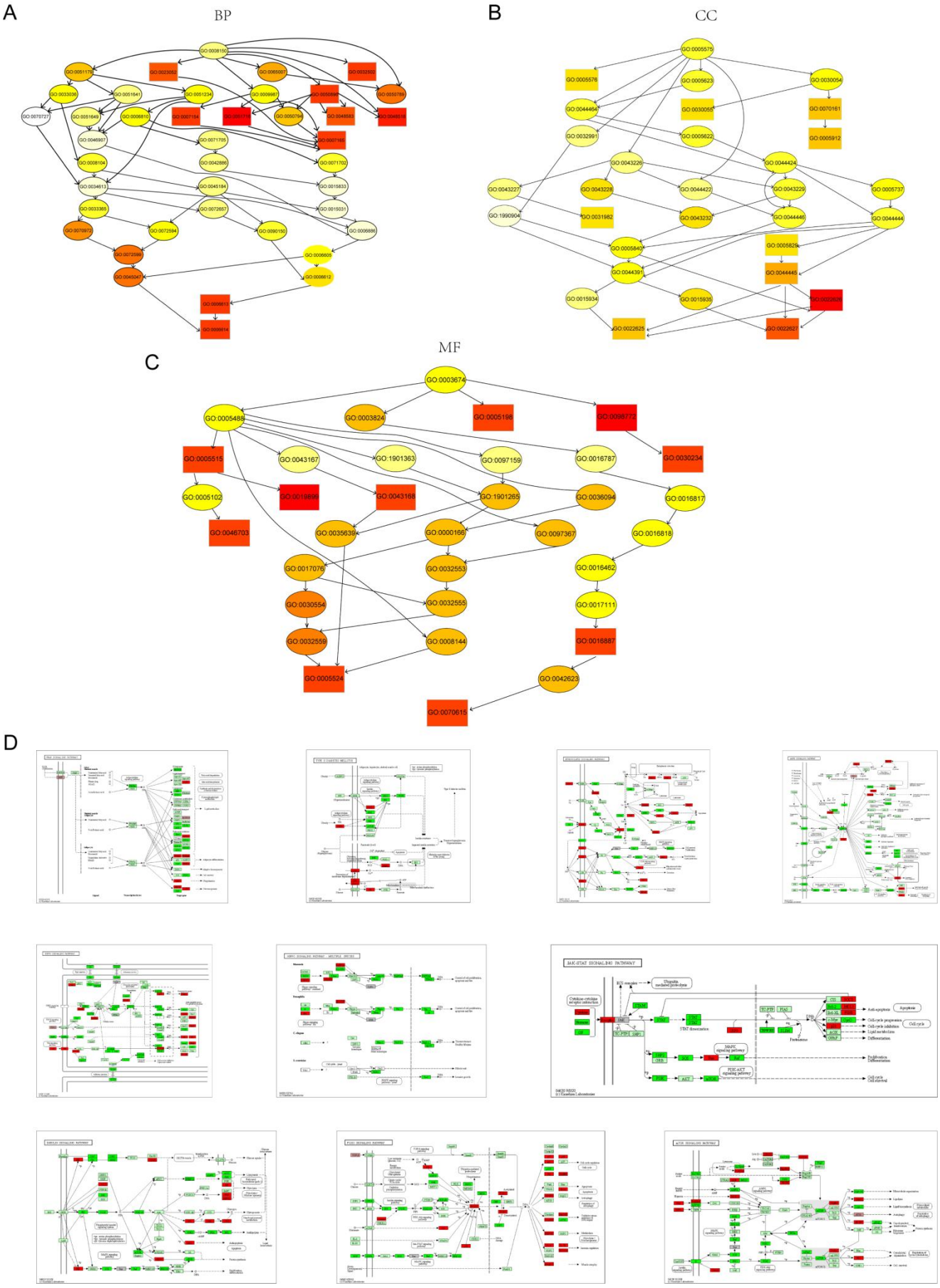
In this study, we discovered that BAZ2A is highly expressed in cervical cancer. Moreover, the reduction of BAZ2A levels inhibited multiple malignant behaviors in HeLa cells, indicating that it plays a significant role in the growth and metastasis of cervical cancer cells. Transcriptome

analysis identified 6825 differentially expressed genes, which were significantly enriched in processes related to glycolipid metabolism. Additionally, GO and KEGG analyses unveiled the potential role of BAZ2A in cellular signaling and other aspects.

Metabolomic analysis identified a variety of differential metabolites related to tumor development, energy metabolism, and signaling in both ionic modes. KEGG analysis further revealed an enrichment of glycolipid metabolism - related pathways. These pathways impact cellular energy and material metabolism and furnish a metabolic foundation for cancer cell proliferation and migration.

Joint transcriptome and metabolome analysis demonstrated that key genes and metabolites in both were jointly implicated in the BAZ2A regulatory network, thereby affecting signaling pathways such as AMPK, FoxO, and mTOR. These pathways indirectly regulate glycolipid metabolism and consequently influence tumor development. Therefore, we hypothesize that BAZ2A may influence cell proliferation and migration via metabolic reprogramming, which subsequently impacts tumorigenesis and development.

Appendix



Supplementary figure 1. BAZ2A Transcriptome Analysis

Notes: (A - C) Directed acyclic graphs illustrating GO analysis of differentially expressed proteins (DEP) in biological process (BP) (A), molecular function (MF) (C), and cellular component (CC) (B). (D) KEGG pathway annotation map for differential expression analysis.

Institutional Review Board Statement:

The manuscript does not contain clinical studies or patient data.

Acknowledgments:

The author expresses gratitude for the assistance provided by Shanghai Zhongke New Life Biotechnology Co., Ltd.

Funding:

This work was primarily supported by the Central Government Guides Local Science and Technology Development Fund Projects, China (246Z7740G).

Data Availability Statement::

The data that support the findings of this study are available from the corresponding author upon reasonable request.

Author Contributions:

L. Y, W. Q and Z. H conceived and designed the study. H. F and Z. B prepares experimental materials. X. R analyzed the data. X. R wrote the manuscript. X. R, D. L and L. W confirm the authenticity of all the raw data. All authors read and approved the final manuscript.

Informed Consent Statement:

All patients provided their informed consent.

Conflict of Interest:

The authors declare no competing interests.

References

Aktary, Z., Alaee, M., & Pasdar, M. (2017). Beyond cell-cell adhesion: Plakoglobin and the regulation of tumorigenesis and metastasis . Oncotarget , 8(19), 32270–32291.

Anosova, I., Melnik, S., Tripsianes, K., Kateb, F., Grummt, I., & Sattler, M. (2015). A novel RNA binding surface of the TAM domain of TIP5/BAZ2A mediates epigenetic regulation of rRNA genes . Nucleic Acids Research , 43(10), 5208–5220.

Bevill, S. M., Olivares-Quintero, J. F., Sciaky, N., Golitz, B. T., Singh, D., Beltran, A. S., et al. (2019). GSK2801, a BAZ2/BRD9 Bromodomain Inhibitor, Synergizes with BET Inhibitors to Induce Apoptosis in Triple-Negative Breast Cancer . Molecular Cancer Research , 17(7), 1503–1518.

Bortoluzzi, A., Amato, A., Lucas, X., Blank, M., & Ciulli, A. (2017). Structural basis of molecular recognition of helical histone H3 tail by PHD finger domains . The Biochemical

Journal , 474(10), 1633–1651.

Bray, F., Ferlay, J., Soerjomataram, I., Siegel, R. L., Torre, L. A., & Jemal, A. (2018). Global cancer statistics 2018: GLOBOCAN estimates of incidence and mortality worldwide for 36 cancers in 185 countries . CA: A Cancer Journal for Clinicians , 68(6), 394–424.

Dalle Vedove, A., Cazzanelli, G., Batiste, L., Marchand, J. R., Spiliotopoulos, D., Corsi, J., et al. (2022). Identification of a BAZ2A-Bromodomain Hit Compound by Fragment Growing . ACS Medicinal Chemistry Letters , 13(9), 1434–1443.

GLi, C., Wu, W., Ding, H., Li, Q., & Xie, K. (2018). The transcription factor 7 like 2-binding protein TIP5 activates β-catenin/transcription factor signaling in hepatocellular carcinoma . Molecular Medicine Reports , 17(6), 7645–7651.

Grier, D. G., Thompson, A., Kwasniewska, A., McGonigle, G. J., Halliday, H. L., & Lappin, T. R. (2005). The pathophysiology of HOX genes and their role in cancer . The Journal of Pathology , 205(2), 154–171.

Gu, L., Frommel, S. C., Oakes, C. C., Simon, R., Grupp, K., Gerig, C. Y., et al. (2015). BAZ2A (TIP5) is involved in epigenetic alterations in prostate cancer and its overexpression predicts disease recurrence . Nature Genetics , 47(1), 22–30.

Hanahan, D., & Weinberg, R. A. (2011). Hallmarks of cancer: the next generation . Cell , 144(5), 646–674.

Jiao, L., Liu, Y., Yu, X. Y., Pan, X., Zhang, Y., Tu, J., et al. (2023). Ribosome biogenesis in disease: new players and therapeutic targets . Signal Transduction and Targeted Therapy , 8(1), 15.

Johnson, C. A., James, D., Marzan, A., & Armaos, M. (2019). Cervical Cancer: An Overview of Pathophysiology and Management . Seminars in Oncology Nursing , 35(2), 166–174.

Katanaev, V. L., Kryuchkov, M., Averkov, V., Savitsky, M., Nikolaeva, K., Klimova, N., et al. (2020). HumanaFly: high-throughput transgenesis and expression of breast cancer transcripts in Drosophila eye discovers the RPS12-Wingless signaling axis . Scientific Reports , 10(1), 21013.

Li, H., Fang, H., Chang, L., Qiu, S., Ren, X., Cao, L., et al. (2021). TC2N: A Novel Vital Oncogene or Tumor Suppressor Gene In Cancers . Frontiers in Immunology , 12, 764749.

Liu, J., Ren, L., Li, S., Li, W., Zheng, X., Yang, Y., et al. (2021). The biology, function, and applications of exosomes in cancer . Acta Pharmaceutica Sinica. B , 11(9), 2783–2797.

Liu, Y., Wang, J., Guo, J., Zhang, Q., Wang, S., Hu, F., et al. (2024). *Pan-cancer and multi-omics analyses revealed the diagnostic and prognostic value of BAZ2A in liver cancer*. Scientific Reports , 14(1), 5228.

Liu, Y., Wang, S. Q., Long, Y. H., Chen, S., Li, Y. F., & Zhang, J. H. (2016). KRASG12 mutant induces the release of the WSTF/NRG3 complex, and contributes to an oncogenic paracrine signaling pathway . Oncotarget , 7(33), 53153–53164.

Liu, Y., Zhang, Y. Y., Wang, S. Q., Li, M., Long, Y. H., Li, Y. F., et al. (2020). WSTF acetylation by MOF promotes WSTF activities and oncogenic functions . Oncogene , 39(27), 5056–5067.

Masters, J. R. (2002). HeLa cells 50 years on: the good, the bad and the ugly . Nature Reviews. Cancer , 2(4), 315–319.

Neoh, G. K. S., Tan, X., Chen, S., Roura, E., Dong, X., & Gilbert, R. G. (2024). Glycogen metabolism and structure: A review . Carbohydrate Polymers , 346, 122631.

Pecoraro, A., Pagano, M., Russo, G., & Russo, A. (2021). Ribosome Biogenesis and Cancer: Overview on Ribosomal Proteins . International Journal of Molecular Sciences , 22(11), 5496.

Pietrzak, K., Kuzyakiv, R., Simon, R., Bolis, M., Bär, D., Aprigliano, R., et al. (2020). TIP5 primes prostate luminal cells for the oncogenic transformation mediated by PTEN-loss . Proceedings of the National Academy of Sciences of the United States of America , 117(7), 3637–3647.

Putarjunan, A., & Torii, K. U. (2016). Stomagenesis versus myogenesis: Parallels in intrinsic and extrinsic regulation of transcription factor mediated specialized cell-type differentiation in plants and animals . Development, Growth & Differentiation , 58(4), 341–354.

Siegel, R. L., Giaquinto, A. N., & Jemal, A. (2024). Cancer statistics, 2024 . CA: A Cancer Journal for Clinicians , 74(1), 12–49.

Stanley, P. (2011). Golgi glycosylation . Cold Spring Harbor Perspectives in Biology , 3(4), a005199.

Sung, H., Ferlay, J., Siegel, R. L., Laversanne, M., Soerjomataram, I., Jemal, A., et al. (2021). Global Cancer Statistics 2020: GLOBOCAN Estimates of Incidence and Mortality Worldwide for 36 Cancers in 185 Countries . CA: A Cancer Journal for Clinicians , 71(3), 209–249.

Tallant, C., Valentini, E., Fedorov, O., Overvoorde, L., Ferguson, F. M., Filippakopoulos, P., et al. (2015). Molecular basis of histone tail recognition by human TIP5 PHD finger and bromodomain of the chromatin remodeling complex NoRC . Structure , 23(1), 80–92.

Xu, H. H., Yan, W. H., & Lin, A. (2020). The Role of HLA-G in Human Papillomavirus Infections and Cervical Carcinogenesis . Frontiers in Immunology , 11, 1349.

Zhang, X., Xia, F., Zhang, X., Blumenthal, R. M., & Cheng, X. (2024). C2H2 Zinc Finger Transcription Factors Associated with Hemoglobinopathies . Journal of Molecular Biology , 436(7), 168343.

Zou, Z., Tao, T., Li, H., & Zhu, X. (2020). mTOR signaling pathway and mTOR inhibitors in cancer: progress and challenges . Cell & Bioscience , 10, 31.